Regional lung spirometry

RP Clauss
MBChB, MMed (Nuc Med), MD

W Pilloy
MBChB, MMed (Nuc Med), MD

Nuclear Medicine Department, Medical University of Southern Africa

Abstract

Forty consenting patients took part in a study to determine lobar, segmental and regional lung volumes and flows as reflected by changes in lung radioactivity measured by nuclear medicine techniques. Two hundred MBq of the gaseous radioisotope ^{133}Xe were injected into a re-breathing circuit spirometer with an 8 litre capacity and an equilibrium activity of 25 MBq/litre. A posterior dynamic acquisition of 400 frames at 0.125 seconds per frame for the determination of lung volumes and flows was completed, followed by a gas washout period.
The acquisition recorded both tidal breathing and 3-6 cycles of maximal inhalation and exhalation after homogenous mixing of the radioactive Xenon inside the lungs and the spirometer, but before significant diffusion of the tracer into the blood.
The conversion from millilitres to counts was accomplished by matching a representative breath cycle on the spirometric graph with the same cycle on the radioactivity curve generated on the processed scintigram of the whole lung. A change in volume was hence matched to a change in radioactivity, and a specific radioactivity per millilitre of lung volume was calculated.
A region of interest was drawn on the scintigram over a lung lobe or segment. The regional radioactivity change represented a regional breath cycle in this area, with regional volume and flow changes.
Spirometric parameters such as lobar vital capacity, tidal volume, residual volume and forced expiratory volume after 1 second were derived by using the previously calculated radioactivity per millilitre of lung volume.
Total lung volumes and flows derived from radioactivity changes were compared to the concurrent volumes and flows measured on the attached spirometer, and a close correlation was found.

Introduction

Conventional lung function tests measure the combined volumes and flows of both lungs and compare them to established normal values for the investigated population. This measurement is however insensitive to lobar or regional functional changes that may occur with localized pathology.

Hamilton *et al*,[1] applied a mathematical model to tidal breathing, using ^{81m}Kr, and Wernly *et al*[2] predicted postoperative lung function from preoperative lung function tests by weighting these results according to the preoperative lung distribution of ^{99m}Tc MAA and ^{133}Xe. Amis *et al*[3] calculated a flow/volume ratio for specific lung regions in patients with diaphragmatic paralysis using ^{81m}Kr and ^{85m}Kr concentrations at tidal breathing. Holli *et al*[4] and Miörner[5] used computerised multidetector radiospirometric methods to determine regional lung function. Kauppinen-Walin *et al*[6] used similar techniques to compare ^{133}Xe radiospirometry with Helium spirometry and whole-body plethysmography in the determination of functional residual capacity and the effect of body position on this parameter. Secker-Walker *et al*[7] calculated regional lung ventilation from mean functional air exchange in selected lung regions. The above tests measure lung function either indirectly or make use of specialized equipment or isotopes that are not generally available. The aim of this study was to ratify a simple and reproducible method to measure lung function by radioisotopes, for application to small lung regions such as lung lobes or segments.

Using the radiospirometric method described below, lung function was derived from gaseous lung ^{133}Xe

to page 22

from page 21

radioactivity, as measured by an Anger gamma camera that is readily available in any nuclear medicine department. The radioactivity was correlated with the actual lung function, as measured on a concurrently generated spirometric volume curve.

Method

Investigations were performed on 40 consenting patients. Thirty-one were males and nine were females. Ages ranged between 12 and 73 years.

Two hundred MBq of ^{133}Xe gas was introduced into a lead-shielded, re-breathing circuit bell spirometer, where it was homogeneously mixed with ambient air. The capacity of the spirometer was 8 litres and the activity of its gas mixture was 25 MBq per litre.

The patient was connected to the spirometer and proceeded with 5-10 tidal breathing cycles to achieve a dynamic equilibrium between the lung and spirometer gas concentrations (Figure 1).

Four hundred images of 0.125 seconds each were recorded over the lung from a posteriorly positioned Anger gamma camera while the patient continued with tidal breathing, followed by 3-6 maximal forced inhalations and exhalations before the end of the recording. The patient then continued with tidal breathing to wash the gas mixture out of the lungs.

The whole investigation and washout was completed in less than 3 minutes. Measurements were completed before any significant diffusion of the tracer into the blood.

The lung radioactivity graph that was recorded by the gamma camera was compared to the concurrent volume graph that was recorded by the spirometer. A specific radioactivity per unit volume was then calculated:

$$\text{Count/millilitre} = \frac{\text{Change in lung radioactivity over any breathing cycle}}{\text{Change in lung volume over the same breathing cycle}}$$

Once a count/lung millilitre was available, a region of interest could be outlined on the lung scinti-image and radioactivity changes in this region could be expressed as volume changes. For instance, if a lung lobe was outlined on the scinti-image, a total volume for this lobe could be derived. Similarly any lobar volume changes, for instance lobar tidal breathing or maximal inhalation and exhalation volumes for lobar vital capacity could be measured. Hence it was possible to derive lobar spirometric parameters (volumes and flows).

The following spirometric parameters were correlated with total lung radioactivity changes: Tidal volume (TV), vital capacity (VC), expiratory reserve volume (ERV), inspiratory capacity (IC) and forced expiratory volume after 1 second (FEV1).

Other parameters that were measured but not correlated were: residual capacity, FIV 0.5, FIV 1, FIV 3, FEV 0.5 and FEV 3.

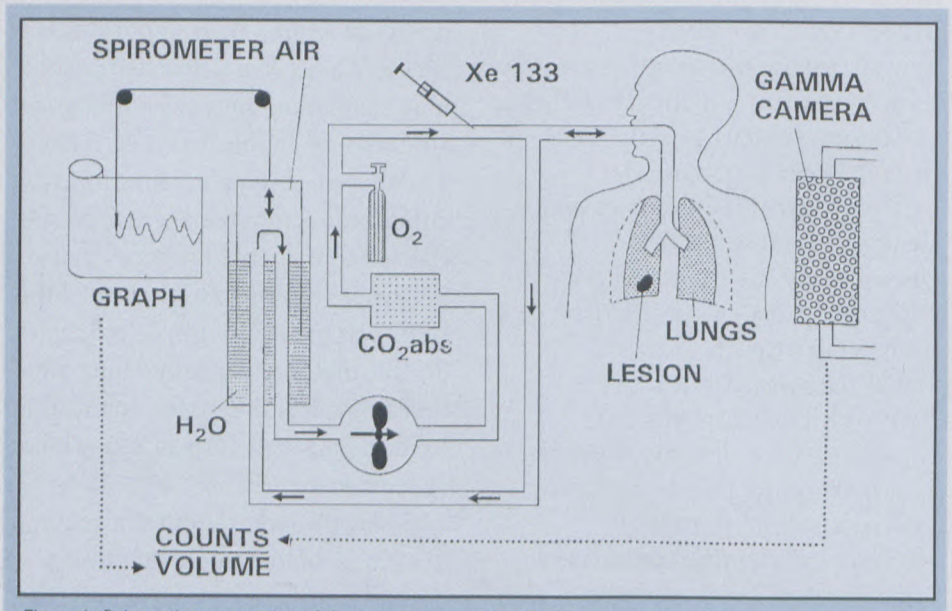

Figure 1: Schematic presentation of the apparatus used for the ^{133}Xe radiospirometry.

Results

Figure 2 shows the graph of radioactivity changes over both lungs while performing tidal breathing and during a number of maximal inhalation and exhalation cycles in a patient with empyaema. Table I shows the correlation of radioactivity to the volume changes in the tested patients.

Discussion

There is a good correlation between spirometric parameters and lung parameters derived from radioactivity changes.

We used the method for determination of regional lung function in various groups. For instance, we compared the function of the affected lung in patients with unilateral haemo- or pneumothorax, before and after physiotherapy. A significant improvement in unilateral lung function was detected after physiotherapy, while total lung function before and after physiotherapy did not change.[8] This

to page 23

from page 22

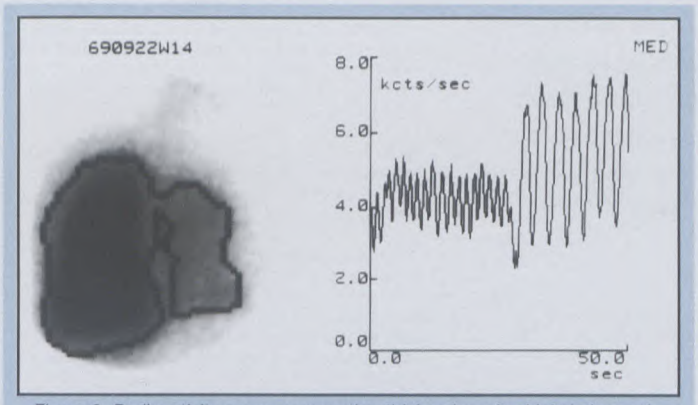

Figure 2: Radioactivity curve representing tidal and maximal inhalation and exhalation manoeuvres.

Table I: Comparison of total lung radiospirometry and concurrent conventional spirometry (n=40)

Parameters (ml)		Mean	Std. dev.	Spearman correlation rr	p
Tidal volume	^{133}Xe	605	252	0.905	0.0001
	Conv.	540	222		
Vital capacity	^{133}Xe	1941	860	0.912	0.0001
	Conv.	1768	616		
Exp. Reserve	^{133}Xe	348	218	0.887	0.0001
	Conv.	334	212		
Insp. Capacity	^{133}Xe	1593	758	0.884	0.0001
	Conv.	1328	498		
FEV1	^{133}Xe	1187	551	0.882	0.0001
	Conv.	1081	368		

was due to compensation by the healthy lung for the incapacitated lung. We have also applied the method to preoperative empyaema patients to predict postoperative lung function.

The determination of regional lung function may be more important than is generally realized. Conventional lung function tests show only global air movements. When the same air movements are followed onto a regional level, it appears that there are ongoing dynamic regional changes in air flows and pressures. For example, while most segments decrease their volumes during expiration, there are some segments that may actually increase their volume. However, these small paradoxical discrepancies cannot be seen on conventional spirometric curves. For example, regional flow/volume loops were generated over the left and the right lungs of one of our patients with bullous lung disease. In this patient, air was shunted from the left lung to the right during an expiratory cycle. Such shunting was however not apparent on the global (total lung) flow/ volume loop (Figure 3).

On the practical side, there are some pitfalls that have to be borne in mind. Xenon is a gas that diffuses from the lung into the blood.[9] Hence, the longer radio-Xenon is in the lung, the more background activity is present in the blood. This may lead to an over-estimation of the residual volume. As the spirometer is a closed circuit, accumulation of CO_2 could occur; this is however absorbed by soda lime crystals in the circuit. The clinical condition of the patient should allow co-operation during tidal breathing and maximal inspiratory and expiratory manoeuvres. Non co-operation may result in leakage of the radioactive gas from the patient's mouth into the surrounding air. When using a bell/fluid spirometer, spillage of water into the spirometer pipes may occur. This results in poor gas mixing and may give misleading results. The piping of the spirometer should therefore be regularly inspected, together with routine calibration.

Another aspect that appears to influence the spirometric curves is the inertia of the spirometer bell. The radioactivity changes and curve edges are sharper and better defined than those on the spirometric graph. Volume changes and the rate of volume change may be under-estimated by conventional spirometry.

The smallest lung region size that could be reasonably evaluated by the above method was approximately 20 ml. In smaller regions, there is a problem of insufficient count statistics.

We are at the moment modifying our techniques to obtain list mode

Figure 3:

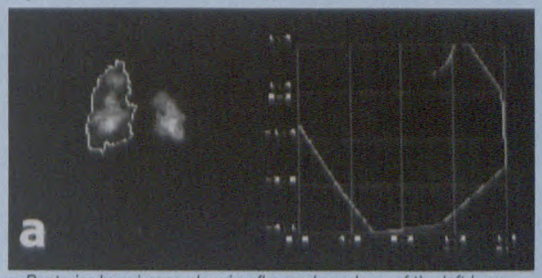

a. Posterior lung image showing flow-volume loop of the left lung starting at high volume and ending at low volume.

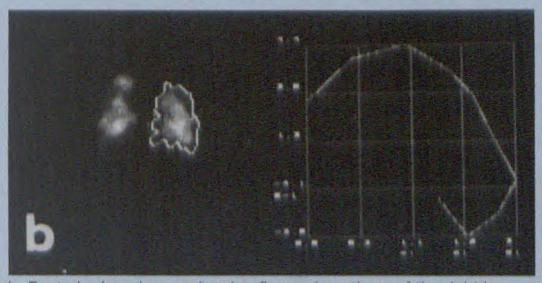

b. Posterior lung image showing flow-volume loop of the right lung starting at low volume and ending at high volume.

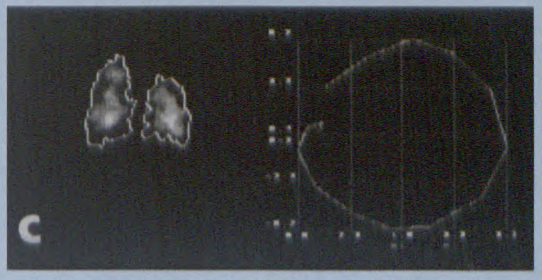

c. Posterior lung image showing the flow-volume loop of both lungs (excluding trachea).

to page 24

Regional lung spirometry

from page 23

rather than frame mode acquisitions, so that framing time can be chosen by the processing operator after completion of the radiospirometry. This helps in the smoothing of curves and in the selection of the activity peaks that are used for determination of lung parameters.

Conclusion

The above method is practical and can be applied in any nuclear medicine department. There is a good correlation between conventional spirometry and ^{133}Xe radiospirometry. There should be further exploration of paradoxic lobar and segmental air movements and investigation into possible local lung reflexes. Regional inco-ordination of such air movements may influence respiratory disease.

References

1. Hamilton D, Godfrey KR, Causer DA, McIntosh JA. Regional specific mean expiratory gas flow from ^{81m}Kr equilibrium inhalation data. *Eur J Nucl Med* 1985;**10**:321-331.
2. Wernly JA, DeMeester TR, Kirchner PT, Myerowitz P, Oxford DE, Golomb HM. Clinical value of quantitative ventilation-perfusion lung scans in the surgical management of bronchogenic carcinoma. *J Thorac Cardiovasc Surg* 1980;**80**:535-543.
3. Amis TC, Ciofetta G, Hughes JMB, Loh L. Regional lung function in bilateral diaphragmatic paralysis. *Clinical Science* 1980;**59**:485-492.
4. Holli H, Muittari A, Paakkala T, Poyhonen L, Seppanen A, Uusitalo A. Comparison between conventional examinations and radiospirometry measured by computerized multidetector unit- Kefut B1 1200 in evaluations of regional lung function pre-operatively and after cobalt therapy. *Radioakt Isop Klin Forsch* 1976;12:23.
5. Miörner G. ^{133}Xe Radiospirometry: A clinical method for studying lung function. *Scand J Respir Dis* 1968;Suppl **64**:17-43.
6. Kauppinen-Walin K, Sovijarui ARA, Muittari A, Uusitalo A. Determination of residual capacity with ^{133}Xenon radiospirometry. Comparison with whole body plethysmography and Helium spirometry. Effect of body position. *Scand J Clin Lab Invest* 1980;**40**:347-354.
7. Secker-Walker RH, Hill RI, Markham J, Baker J, Wilhelm J, Alderson PO, Potchen EJ. The measurement of regional ventilation in man: A new method of quantification. *J Nuc Med* 1973;**14**:725-731.
8. Mji M, Clauss RP. The effects of expiratory and incentive expiratory spirometry on young males with traumatic haemo-pneumo-thorax. MEDUNSA abstracts 1991;12th academic day.
9. Ahmad M, Perrillo RP, Sunwoo YC, Donati RM. Xenon-133 retention in hepatic steatosis - correlation with liver biopsy in 45 patients: concise communication. *JNM* 1979;**20(5)**:397-401.

from page 15

A mini review of paragangliomas with presentation of two cases

Surgical cure rates of 66-85 % have been reported with a 5-10 % recurrence rate.[2,3] The five year survival is 80-95 % with surgery, and less than 50 % in malignant disease.[2,13] The hypertension cure rate is 75 % if total tumour excision is accomplished. In 25 % of cases the hypertension persists either due to unmasking of primary hypertension, intraoperative renal ischaemia, damage to the renal vessels, or catecholamine-induced vascular damage.

Conclusion

Paragangliomas are rare tumours that are potentially lethal if undiagnosed or discovered incidentally. Their early diagnosis requires a high index of suspicion and appropriate biochemical tests. Accurate radiological localisation of the tumour is best accomplished using MRI as a first line investigation with MIBG scans being reserved for cases of recurrence, multicentricity, metastatic disease or equivocal MRI. Where the tumour is biochemically inactive, MRI scanning is the best option. Octreotide is emerging as a promising agent, but its long-term performance remains to be fully evaluated. Appropriate and early intervention carries a favourable prognosis in an otherwise dangerous tumour.

Acknowledgements

The author wishes to thank Prof S Beningfield for his assistance in the preparation of this review, Dr P Szkup for the use of illustrative figures and Miss L Heyburgh for manuscript preparation.

References

1. Van Gils APG, Van Erkel AR, Falke THM. *et al.* Magnetic Resonance Imaging or Metaiodobenzylguanidine scintigraphy for the demonstration of paragangliomas? *European Journal of Nuclear Medicine* 1994; **21(3)**: 239-253.
2. Wilson, Braunwald, Isselbacher, Petersdorf *et al. Harrison's Principles of Internal Medicine* 12th ed. McGraw-Hill 1991: 1735-1739.
3. Felig, Baxter, Frohman. *Endocrinology and Metabolism.* 3rd ed. McGraw-Hill 1995: 713-731.
4. Williams, Warwick, Dyson *et al. Grays Anatomy* 37th ed. Churchill Livingstone 1987: 200,201,1465-1467.
5. O'Riordain DS, Young WF, Grant CS *et al.* Clinical spectrum of functional extra-adrenal paraganglioma. *World Journal of Surgery* 1996; **20(7)**: 916-921.
6. Dunn GD, Brown MJ, Sapsford RN *et al.* Functioning middle mediastinal paraganglioma associated with intercarotid paraganglioma. *Lancet* 1986; **(I)**: 1061-1064.
7. Rehm A, Williams RJ. Case report: an intra-abdominal tumour. *Post Graduate Medical Journal* 1997; **73(860)**: 353-355.
8. Hayes WS, Davidson AJ, Grimley PM *et al.* Extra-adrenal retroperitoneal paraganglioma: clinical pathological and CT findings. *American Journal of Roentgenology* 1990; **155(6)**: 1247-1250.
9. Kwekkeboom DJ, Van Urk H, Pauw BKH *et al.* Octreotide scintigraphy for the detection of paragangliomas. *Journal of Nuclear Medicine.* 1993; **34(6)**: 873-878.
10. Grainger RG, Allison DJ. *Diagnostic Radiology* 3rd ed. Churchill Livingstone 1997: 293-294, 2451.
11. Bloodworth J. *Endocrine Pathology - general and surgical.* 2nd ed. Williams and Williams 1981: 482-505.
12. Harach HR, Wheatley T, Smellie WAB *et al.* Phaeochromocytoma of the organ of Zuckerkandl invading the inferior vena cava. *Histopathology.* 1996; **28(6)**: 556-559.
13. Altergott R, Barbato A, Lawrence A et al. Spectrum of catecholamine-secreting tumours of the organ of Zuckerkandl. *Surgery* 1985-98; **(6)**: 1121-1126.
14. Shapiro B, Copp JE, Sisson JC *et al.* Iodine 131 metaiodobenzylguanidine for the locating of suspected phaeochromocytoma: experience in 400 cases. *Journal of Nuclear Medicine* 1995; **26**: 576-585.
15. Maurea S, Cuocolo A, Reynolds JC *et al.* I^{131} MIBG scintigraphy in preoperative and postoperative evaluation of paragangliomas: comparison with CT and MRI. *Journal of Nuclear Medicine* 1993; **34(1)**: 173-179.
16. Schmedtje JF, Sax S Pool JL *et al.* Localisation of ectopic phaeochromocytoma by Magnetic Resonance Imaging. *American Journal of Medicine* 1987; **83**: 770-772.
17. Van Gelder T, Verhoeven GT, de Jong P *et al.* Dopamine producing paraganglioma not visualised by I^{123} scintigraphy. *Journal of Nuclear Medicine* 1995; **36(4)**: 620-622.